Arch. Mech., 41, 6, pp. 867–893, Warszawa 1989

Space-time element method in structural dynamics

CZ. BAJER (WARSZAWA) and A. PODHORECKI (BYDGOSZCZ)

THE PAPER deals with recent developments of the space-time element method in vibration analysis. Discrete methods applied to date in structural dynamics make use of spatial discretization independently of the time integration procedure. It limits applications of such an approach. The full space-time approximation can be considered as an extension of the finite element method over the time domain and it allows to treat spatial variables in the same way as the time variable. Nonstationary discretization, adaptive techniques, directly obtained joint-by-joint procedure are not the only positive features of the space time finite element approach. Although the additional time variable in the shape functions is considered and the resulting element matrices are greater than static stiffness and mass matrices, the cost of the solution algorithm is comparable with other numerical methods. Some testing examples prove the efficiency of the method.

Omówiono ostatnie osiągnięcia w dziedzinie zastosowania metody elementów czasoprzestrzennych w analizie drgań. Stosowane dotąd dyskretne metody analizy dynamicznej konstrukcji zakładają przestrzenną dyskretyzację niezależną od procedury całkowania równania różniczkowego ruchu w czasie. Takie przyjęcie znacznie ogranicza zastosowania. Pełna czasoprzestrzenna aproksymacja rozumiana jest jako rozszerzenie na zmienną czasową metody elementów skończonych i umożliwia rozpatrywanie czasu w taki sam sposób, jak zmiennych przestrzennych. Niestacjonarna dyskretyzacja, techniki adaptacyjne, bezpośrednio uzyskana procedura obliczeniowa „węzeł po węźle" nie są jedynymi zaletami podejścia czasoprzestrzennego. Chociaż uwzględnia się dodatkową zmienną czasową w funkcjach kształtu i otrzymuje się większy wymiar wynikowych macierzy elementu od wymiarów statycznych macierzy sztywności czy mas, to koszt algorytmu obliczeniowego jest porównywalny z kosztem innych metod numerycznych. Zamieszczone przykłady obliczeniowe wykazują skuteczność przedstawionej metody.

Работа обсуждает последние достижения в области применения метода времени- пространственных элементов в анализе колебаний. Применяемые до сих пор дискретные методы динамического анализа конструкций предполагают пространственную дискретизацию независимую от процедуры интегрирования дифференциального уравнения движения во времени. Такой подход значительно ограничивает присменения. Полная времени-пространственная аппроксимация понимается как расширение на временную переменную метода конечных элементов и дает возможность рассматривать время таким самым образом как пространственные переменные. Нестационарная дискретизация, адаптационные техники, непосредственно полученная расчетная процедура „узел за узлом" не являются единственными достоинствами времени-пространственного подхода. Хотя учитывается дополнительная временная пер менная в функциях формы и получается размер результирующих матриц элемента больше чем размеры статических матриц жесткости или масс, то стоимость расчетного алгоритма сравнителен со стоимостью других численных методов. Помещенные расчетные примеры показывают эффективность представленного метода.

1. Introduction

STUDIES in the field of the space-time element method (STEM) have been carried out for several years. In this time considerable progress in direct time integration methods has been made. Time integration has been applied both to linear and nonlinear problems.

The elliptic part of the differential motion equation is treated in spatial domain by any discrete method (finite element, finite difference or other) while the time derivative is approximated by the difference rule. Such an approach was commonly used since all the algorithms applied to statics could be directly adapted for dynamics. The domain of research was split into two: exclusively the spatial approximation, new models of finite elements, new methods for static solutions, was in the scope of the first group while time marching schemes, their accuracy and efficiency were developed in the second group. The separate approach to spatial and time variable could be considered as a simplification with natural limitations that make it impossible to solve some problems in a natural way. The example of the problem that could not be treated with sufficient simplicity is the movable mesh case in elastodynamics.

The first attempts of a complex treatment of vibrating structures in space and time did not give either numerical savings or possibilities of new solutions. Even more, in classical problems the space-time element approach was time and memory consuming. This fact propagated the negative opinion on the STEM [1]. In spite of this, research was conducted by an increasing group of people. However, three general achievements must be pointed here. The first is the use of simplex-shaped elements that considerably reduces the cost of the method. The second is the nonstationary partition of the structure that enables to adapt the mesh to the local error value (r-adaptation). The third is the development of the method towards nonlinear problems.

Besides the continuous in time approximation between two successive layers, the second, highly interesting approach of noncontinuous approximation has been recently published by HUGHES and HULBERT [2]. The Petrov–Galerkin method in a mean of least squares is the base of the solution. Discontinuity from layer to layer is admitted while the energy criterion must be balanced in each time layer.

In the paper the recent achievements in the field of the STEM are presented. More detailed considerations exhibit state-of-the art in the field.

2. Basic formulation of the method

2.1. Fundamental research

The possibility of generation of finite elements in space and time was noticed in early papers by FRIED, ODEN, ARGYRIS, SHARPF and CHAN [3–7]. The subject can also be found in the monographic work by ZIENKIEWICZ [8] and [9]. These considerations influenced KĄCZKOWSKI to work out the original method of the space-time finite elements [10, 11]. The discretization of the space-time continuum resulting in the one-stage path from the differential equations to the algebraic ones is the basic idea of the approach. The characteristic feature that differs the STEM from other time integration methods is the characteristic approximation of the displacement, strain and stress field in the whole considered space-time domain. For example, the displacement function in the space-time element is described with respect to the nodal parameters r

$$\mathbf{u}^e(\mathbf{x}, t) = \Phi(\mathbf{x}, t)\mathbf{r}_e, \tag{2.1}$$

where $\Phi(\mathbf{x}, t)$ is the interpolation function (shape function) that depends on the spatial coordinates and time coordinate. In the classical time integration schemes, we use, for example, the finite element approximation to space:

$$\mathbf{u}^e(\mathbf{x}, t) = \Phi(\mathbf{x})\mathbf{r}_e(t). \tag{2.2}$$

It converts the system of the partial differential equations to the system of the ordinary differential equations depending on time which can be solved by different numerical methods. The possibility of separate discretization of space and time is the advantage of the assumption (2.2). However, the basic disadvantage is that the initially-assumed spatial partition cannot be changed in time. In the full space-time approach such a restriction does not exist. The discretization is not limited and enables to adjust the spatial partition to the load function or varying boundary and to solve the nonlinear problems in which vibrations of the structure fulfil different equations in passing time.

Studies on the space-time field are broad. The early works by KĄCZKOWSKI [10–12] were devoted to the basic space-time terms. The equation of the time-work was formulated and the rules of the space-time element matrix generation were presented. In the following papers several problems of linear structural dynamics were solved [13–21]. In [22] KĄCZKOWSKI and LANGER proved that if the rectangular space-time elements are in use, the STEM can be considered as a direct time integration method. The stability problem was discussed in [23–32]. In later works the non-rectangular elements were worked out [26, 33–36]. They enabled nonstationary discretization of the structure and the solution of a new class of problems. Attempts to treat the geometrically nonlinear cases were described in [40, 41]. Thermal problems [42–46], thermoelasticity [47] and viscoelasticity [48–50] were also considered.

2.2. The equation of virtual time-work

We consider a continuous body in a domain V^*, which is a subdomain of the Euclidean space E^3. V denotes the interior of the domain being considered and ∂V — its boundary which is a sum of ∂V_t and ∂V_u (Fig. 1). The motion of the body will be considered in the time interval $[0, T]$. The dynamic variables that appear in the description, i.e., displacement

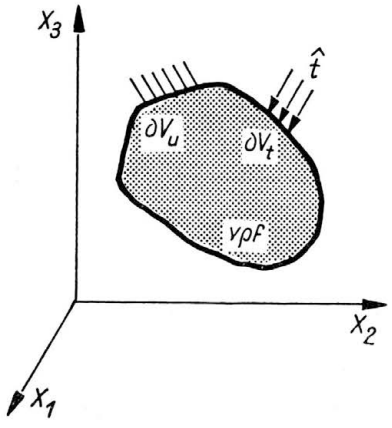

FIG. 1. Notations in elastic body analysis.

vector field $\mathbf{u}$ and mass forces $\varrho\mathbf{f}$, symmetric tensor field of stresses σ and strains ε are described in the Cartesian product of the sets $V\times[0, T]$. The vector field of the surface forces $\hat{\mathbf{t}}$ is described in the product $\partial V\times[0, T]$. All the functions are sufficiently continuous. In the formulation of the equations we use the rules of the tensor calculus.

The unstable, geometrically and physically linear problem is defined by the following set of equations [51]:

a) geometric equations

$$\varepsilon_{ij}(\mathbf{x}, t) = \frac{1}{2}(u_{i,j}+u_{j,i}), \qquad \mathbf{x}, t \in V\times[0, T], \tag{2.3}$$

b) physical equations

$$\sigma_{ij}(\mathbf{x}, t) = C_{ijkl}\varepsilon_{kl}, \qquad \mathbf{x}, t \in V\times[0, T], \tag{2.4}$$

c) dynamic equilibrium equations

$$\sigma_{ji,j}+\varrho f_i = \varrho\ddot{u}_i, \qquad \mathbf{x}, t \in V\times[0, T], \tag{2.5}$$

d) boundary conditions

$$\sigma_{ji}\nu_j = \hat{t}_i(\mathbf{x}, t), \qquad \mathbf{x}, t \in \partial V_t\times[0, T], \tag{2.6}$$

$$u_i(\mathbf{x}, t) = \hat{u}_i, \qquad \mathbf{x}, t \in \partial V_u\times[0, T], \tag{2.7}$$

e) initial conditions

$$u_i(\mathbf{x}, t) = u_i^0, \qquad \mathbf{x}, t \in V^*\times\{0\}, \tag{2.8}$$

$$\dot{u}_i(\mathbf{x}, t) = v_i^0, \qquad \mathbf{x}, t \in V^*\times\{0\}. \tag{2.9}$$

The above equations describe the local formulation that has the proof of existence and uniqueness of the solution [52]. We can pass to the global formulation by multiplication of Eqs. (2.5) by the virtual variation of the displacement function $\delta\mathbf{u}(\mathbf{x}, t)$:

$$\delta\mathbf{u}(\mathbf{x}, t) = \begin{cases} 0, & \mathbf{x}, t \in \partial V_u\times[0, T], \\ \text{any}, & \mathbf{x}, t \in (V^*-\partial V_u)\times[0, T]. \end{cases} \tag{2.10}$$

After integration over the space-time domain, we have

$$\int_0^{t_1}\int_V \varrho(f_i\delta u_i+\dot{u}_i\delta\dot{u}_i)dVdt+\int_0^{t_1}\int_{\partial V_t}\hat{t}_i\delta u_i d(\partial V)dt + \int_V \varrho\dot{u}_i\delta u_i dV\Big|_0^{t_1} = \int_0^{t_1}\int_V \sigma_{ij}\delta\varepsilon_{ij}dVdt, \qquad t_1 \in [0, T]. \tag{2.11}$$

The above equation must fulfil the conditions (2.3), (2.4) and (2.7).

2.3. Discretization of the space-time domain

We divide the space-time domain $C(\bar{\Omega})$, $\bar{\Omega}$: $\{V, 0 \leqslant t \leqslant T\}$ into finite space-time elements Ω_e, $e = 1, 2, \ldots, E$ (Fig. 2). The shape and number of space-time elements can vary according to the problem to be solved. We assume that the elements are connected with each other in a finite number of points. The nodal parameters state the basic unknown vector. The quantities in Eq. (2.11) are described with the use of nodal displacements

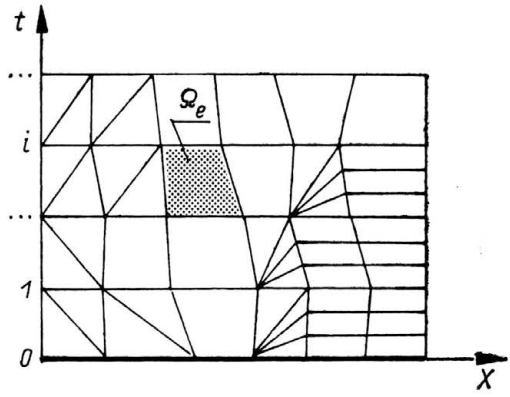

FIG. 2. Example of the space-time mesh.

$$
\begin{aligned}
u_i(\mathbf{X}, t) &= \Phi_{i\alpha}(\mathbf{X}, t)\mathbf{r}_\alpha, & \delta u_i(\mathbf{X}, t) &= \Phi_{i\alpha}(\mathbf{X}, t)\delta\mathbf{r}_\alpha,\\
\dot{u}_i(\mathbf{X}, t) &= \dot{\Phi}_{i\alpha}(\mathbf{X}, t)\mathbf{r}_\alpha, & \delta\dot{u}_i(\mathbf{X}, t) &= \dot{\Phi}_{i\alpha}(\mathbf{X}, t)\delta\mathbf{r}_\alpha,\\
\varepsilon_{ij}(\mathbf{X}, t) &= B_{i\alpha j}(\mathbf{X}, t)\mathbf{r}_\alpha, & \delta\varepsilon_{ij}(\mathbf{X}, t) &= B_{ij\alpha}(\mathbf{X}, t)\delta\mathbf{r}_\alpha,\\
\sigma_{ij}(\mathbf{X}, t) &= C_{ijkl}B_{kl\alpha}(\mathbf{X}, t)r_\alpha,
\end{aligned}
\tag{2.12}
$$

$$
i, j, k, l = 1, 2, 3, \qquad \alpha = 1, 2, \ldots, N
$$

(N — number of nodes in a space-time element multiplied by a nodal number of degrees of freedom), where

$$
B_{ij\alpha} = \frac{1}{2}(\Phi_{i\alpha,j} + \Phi_{j\alpha,i}).
$$

The interpolation functions (shape functions) are assumed in a way typical for the finite element method (for example [8]). Applying the approximation rule (2.11) to Eq. (2.10), we have

$$
\sum_{e=1}^{E} \{\delta\mathbf{r}_\alpha^e[\mathbf{K}_{\alpha\beta}^e\mathbf{r}_\beta^e - \mathbf{R}_\alpha^e]\} = 0, \tag{2.13}
$$

where

$$
\begin{aligned}
\mathbf{K}_{\alpha\beta}^e &= \int\int [C_{ijkl}^e B_{kl\beta}^e B_{ij\alpha}^e - \varrho^e \Phi_{i\alpha}^e \Phi_{ib}^e] d\Omega,\\
\mathbf{R}^e &= \int\int_{\Omega_e} \varrho^e f_i^e \Phi_{i\alpha}^e d\Omega + \int\int_{\partial\Omega_e} t_i^e \Phi_{i\alpha}^e d(\partial\Omega) + \int_{V_e} \varrho^e \dot{u}_i^e \Phi_{i\alpha}^e dV \Big|_{t_{\text{init}}^e}^{t_{\text{end}}^e}
\end{aligned}
\tag{2.14}
$$

denote the space-time element stiffness matrix and the nodal impulse vector, respectively.

Equation (2.13) must be fulfilled for any variation of displacements

$$
\sum_{e=1}^{E} [\mathbf{K}_{\alpha\beta}^e\mathbf{r}_\beta^e - \mathbf{R}_\alpha^e] = \mathbf{0} \tag{2.15}
$$

and for the whole discretized time space. We obtain the system of N linear equations that should be solved for nodal displacements $\mathbf{r}$.

3. Simplex-shaped elements

ODEN in [4] presented the nonstationary partition of the structure. He used quadrangular and tetrahedral forms for a uni-dimensional structure. However, he did not continue his research.

Below we consider the topological properties of triangles, tetrahedrons and hypertetrahedrons, all of them generally called simplex-shaped forms. When we divide the time space into simplex-shaped elements only, we can obtain the triangular coefficient matrix directly during the global matrix assembly. It can also be gained by the row and column change or by special numbering of nodes before the calculation of element matrices. The arbitrary partition and node numbering as well as the special technique give us the expected savings although the second way makes programming easier.

Let us see this on the basis of an example. Follow the steps:

1. Divide the bar structure into finite elements with joint numbering ($t = 0$).
2. Imagine the same partition in $t = \Delta t$; now we have the space-time layer.
3. Consider the first joint (of any number, for example i), join the node in $t = 0$ and its image in $t = \Delta t$ by the line parallel to the time axis.
4. Then consider the neighbouring nodes (let they be j). If $i < j$, then connect $i|_{t=\Delta t}$ and $j|_{t=0}$. If $i > j$, then connect $i|_{t=0}$ and $j|_{t=\Delta t}$.
5. Complete the loop over the neighbouring nodes (return to 4).
6. Complete the loop over the nodes (return to 3).

The above algorithm (illustrated in Fig. 3) is appropriate to any spatial dimensions. In the case of plane structures we only obtain tetrahedrons instead of triangles. More details can be found in [38].

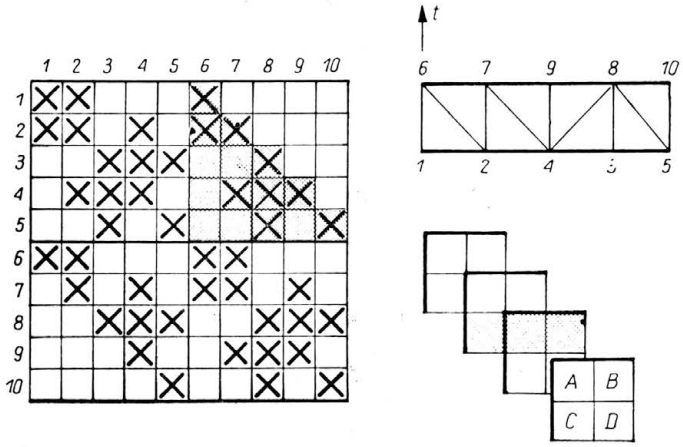

FIG. 3. Global matrix of coefficients for one-time layer.

3.1. Step-by-step solution

There are two possible ways of solving an equation system with variable coefficients.

The first: we assemble the one-layer equation retaining the remaining matrices for use in the next step. We keep the following tables:

$$\begin{matrix} \mathbf{C}_{i-1} & \mathbf{D}_{i-1}+\mathbf{A}_i & \mathbf{B}_i \\ & \mathbf{C}_i & \mathbf{D}_i \end{matrix}$$

Three of them are triangular and two — quandrangular. We obtain $\mathbf{q}_{i+1}$ from the equation

$$\mathbf{B}_i\mathbf{q}_{i+1} = \mathbf{F}_i - \mathbf{C}_{i-1}\mathbf{q}_{i-1} - (\mathbf{D}_{i-1}+\mathbf{A}_i)\mathbf{q}_i \tag{3.1}$$

that is rather fast since $\mathbf{B}_i$ is triangular.

The second: we keep only one triangular matrix $\mathbf{B}_i$, one quadrangular $\mathbf{D}_i$ and one temporary vector $\mathbf{t}_i$ which initially depends on the starting conditions. We solve for $\mathbf{q}_{i+1}$

$$\mathbf{B}_i\mathbf{q}_{i+1} = \mathbf{F}_i - \mathbf{A}_i\mathbf{q}_i - \mathbf{t}_i \tag{3.2}$$

preparing $\mathbf{t}_{i+1}$ for the forthcoming step

$$\mathbf{t}_{i+1} = \mathbf{C}_i\mathbf{q}_i + \mathbf{D}_i\mathbf{q}_{i+1}. \tag{3.3}$$

The products $\mathbf{C}_i\mathbf{q}_i$ and $\mathbf{A}_i\mathbf{q}_i$ can be computed during matrix element calculation. This two-step procedure is similar to the velocity formulation [28]. It is more efficient than the first way of solution considering the memory requirements but it needs more arithmetical operations (multiplications) per one step.

One characteristic property of simplex-shaped elements must be mentioned here. That is the limited speed of wave propagation in the direction of slope edges. A regular mesh with slope sides directed identically shows the anisotropy in time, that is the infinite wave speed in one direction and finite speed in the other. It can be useful in some wave propagation problems, i.e., shocks placed to a point. Isotropic propagation can also be achieved by a special partition.

3.2. Efficiency of one step path

Presently the cost of random access memory decreases considerably so the size of the problem to be solved is rarely limited. However, the time of computations still really limits the size of the task. Usually the number of multiplications is used as a measure of the algorithm cost. When the mathematical coprocessor exists in computer hardware, multiplications are executed with the same speed as additions. It is difficult to assume a good measure of computational effort. Since the total number of operation is proportional to the time consumed in calculations and multiplications are almost a constant percentage of them, we assume the number of multiplications as a measure of efficiency of an algorithm.

Additional time dimension in the space-time element approach results in greater element matrices. For example, in the case of a triangular plane element we compute 36 coefficients. The respective space-time layer filled by 3 tetrahedrons requires 192 coefficients, that is 5.33 times more. This ratio decreases for uni-dimensional structures to 4.50 and reaches 6.25 for the 3-D body.

The question is what gives us the increased computational effort? First of all better space-time approximation of displacements, linear between two successive whiles, instead of the constant one as it is in classical time integration schemes. Adaptive techniques can be applied in a natural way then.

However, the triangular coefficient global matrix requires a smaller number of operations. The simplex space-time element method requires:

1) in the case of the one-step solution scheme

$$M = 2sN(c+1); \tag{3.4}$$

2) in the case of the two-step solution scheme

$$M = 3sN(c+1). \tag{3.5}$$

Here s is a nodal number of degrees of freedom, N — the total number of degrees of freedom in a structure, c — the number of joints which neighbour any joint in the mesh.

As a comparison ([1]) we can look at the estimation of the Newmark and Trujillo method. In the first one we have

$$M = \frac{Nb^2}{2n} + N(4b+3), \tag{3.6}$$

where b — half band width, n — number of time steps.

The Trujillo method ([2]) requires

$$M = 2sN(c+1)+10N \tag{3.7}$$

multiplications.

Memory requirements

Memory requirements are measured as the number of real values L stored in the memory to run the task. In the one-step procedure

$$L = 3.5sN(c+1)+1.5sN \tag{3.8}$$

and in the two-step procedure

$$K = 1.5sN(c+1). \tag{3.9}$$

4. Stability restrictions

Some important problems appear while solving the differential equations by numerical means. A fundamental one is the question how to pose the problem well, i.e., the existence of the unique solution and its continuous dependence on the right-hand side and the boundary conditions. The last property is the stability of the differential problem.

The convergence is the approach of the estimated problem to the original one when the step of integration or the finite element dimension goes to zero. The approximation error is the error caused by the numerical method related to one computational step, without the influence of the previous step error. The estimated problem is stable when small disturbance in right-hand side coefficients results also in small disturbance of the solution. The numerical method is stable when it ensures the solution with the avoidable error

([1]) R. Mullen, T. Belytschko, An analysis of an unconditionally stable explicit method, Comp. Struct., 16, 691–696, 1983.

([2]) D. M. Trujillo, An unconditionally stable explicit algorithm for structural dynamics, Int. J. Num. Meth. Engng., 11, 1579–1592, 1977.

level resulting from the estimated representation of data and results. We can emphasize that the stability of the numerical algorithm is only the necessary condition for the correctness of the numerical method.

There are two reasons for instability of the solution schemes in the STEM. The value of the time step in the integration of the motion equation is the first one. The time step is understood here as a time dimension of the space-time finite element. In the case of non-rectangular elements, it is difficult to express the influence of the time step on the stability. The second reason, the influence of the geometry of the space-time elements, is also difficult to show. Below we will exhibit selected cases of non-rectangular meshes and restrictions imposed on the element geometry.

4.1. General stability condition

The stepping rule can be written with the use of the amplification matrix **T** [32]

$$\mathbf{X}_{i+1} = \mathbf{T}_i\mathbf{X}_i + \mathbf{R}_i, \quad \text{where} \quad \mathbf{X}_i = \begin{Bmatrix} \mathbf{r}_i \\ \dot{\mathbf{r}}_i \end{Bmatrix}. \tag{4.1}$$

The sufficient condition for the stability of the problem (6.1) is

$$\varrho(\mathbf{T}) \leqslant 1 + \alpha\Delta t, \tag{4.2}$$

α — any positive number, $\varrho(\mathbf{T})$ is the spectral radius of the matrix. We can also give the estimation for $\varrho(\mathbf{T})$

$$\varrho(\mathbf{T}) \leqslant \max \sum_{j=1}^{m} |t_{ij}|, \qquad \varrho(\mathbf{T}) \leqslant \sqrt{\operatorname{tr}(\mathbf{T}\mathbf{T}^T)},$$

$$\varrho(\mathbf{T}) \leqslant \sqrt[2m]{\operatorname{tr}(\mathbf{T})^{2m}}.$$

In the investigations we use the system of two elements with end nodes fixed in which only the inner joint can move. The simplest mesh has been used to investigate the influence of only the movement d on the stability criterion. The selection of the type of mesh geometry allows us to treat the worst case. In any other, even more complicated system with a nonstationary joint location, we can expect milder restrictions. Each second layer of nodes was eliminated and in this way reproducible superelements were obtained. The matrix of the system of equations can be written in a block form:

$$\begin{bmatrix} \mathbf{F} & \mathbf{A} & \mathbf{B} & & \\ & \mathbf{C} & \mathbf{D} & \mathbf{E} & \\ & & \mathbf{F} & \mathbf{A} & \mathbf{B} \\ & & & \mathbf{C} & \mathbf{D} & \mathbf{E} \end{bmatrix}.$$

The transfer matrix **T** now has the form

$$\mathbf{T} = \begin{bmatrix} (\mathbf{B}\mathbf{D}^{-1}\mathbf{E})^{-1}(\mathbf{A} - \mathbf{F}\mathbf{D}^{-1}\mathbf{E} - \mathbf{B}\mathbf{D}^{-1}\mathbf{C}) & -(\mathbf{B}\mathbf{D}^{-1}\mathbf{E})^{-1}\mathbf{F}\mathbf{D}^{-1}\mathbf{C} \\ \mathbf{I} & \mathbf{0} \end{bmatrix}. \tag{4.3}$$

4.2. Sample mesh investigations

Below we consider some chosen problems and their stability properties. First we mention the multiplex form of space-time elements. In this case shape functions can be uncoup-

led and only the time variable for one degree of freedom can be considered. Then a bar in axial vibrations solved with quadrangular and triangular elements are investigated. At the end, beam and plane elements are described.

Multiplex elements

Only the time-dependent term of the shape function is modified by the third-order term scaled by a parameter α [28]:

$$\bar{\Phi}_i(\tau) = \frac{1}{2}(1+\tau\tau_i)+\alpha\tau_i(\tau^3-\tau). \tag{4.4}$$

The unconditionally stable scheme can be obtained for $\alpha \geqslant 1.25$.

Quadrangular elements

Shape functions are expressed in a local coordinate system. In this case the element domain becomes a square $\{\xi, \tau: -1 \leqslant \xi \leqslant 1, -1 \leqslant \tau \leqslant 1\}$. Shape functions for real displacements are assumed in the form

$$\Phi_i(\xi, \tau) = \frac{1}{4}(1+\xi\xi_i)(1+\tau\tau_i). \tag{4.5}$$

For virtual displacement we modify the time-dependent part of a shape function $\tilde{\Phi}_i$

$$\tilde{\Phi}_i(\xi, \tau) = \frac{1}{2}(1+\xi\xi_i)\left[\frac{1}{2}(1+\tau\tau_i)+\alpha\tau_i(\tau^3-\tau)\right]. \tag{4.6}$$

The coefficient α modifies the shape function and flows into the element's properties. The influence of the coefficient α on the stability and accuracy of the solution is determined below.

Let us consider an element of a parallelogram shape and lenght b, fixed on one joint's line to eliminate the lower modal frequency. We remember that only the highest frequency determines the stability restrictions. Coefficients of stiffness and mass matrices can be derived analytically. They are such:

$$\begin{aligned} &\frac{1}{EA}K_{ij} = \frac{h}{4b}\xi_i\xi_j\left(1+\frac{5-4\alpha}{15}\tau_i\tau_j\right), \\ &\frac{1}{\varrho A}M_{ij} = -\frac{d}{4h}(\xi_i\tau_j+\tau_i\xi_j)-\frac{\xi_i\xi_j d^2}{4bh}-\frac{\tau_i\tau_j b}{4h}-\frac{\xi_i\xi_j\tau_i\tau_j}{180bh}(15b^2+15d^2-12\alpha d^2). \end{aligned} \tag{4.7}$$

The transient matrix can be formed considering only free joints. The stability condition for the differential stepping scheme leads to the inequality

$$-1 \leqslant \frac{2K^2(5-\alpha)-10(1-k^2)+2\alpha k^2}{(K^2-k^2)(5+2\alpha)+10} \leqslant 1, \tag{4.8}$$

where

$$K = \frac{ch}{b}, \quad k = \frac{d}{b},$$

c — wave speed, $c^2 = E/\varrho$. We also introduce the dimensionless parameter $s = d/hc$.

The coefficient K is the Courant number and can be considered as a shape measure related to the wave speed c. The dimensionless parameter k is a measure of the slope of the parallelogram.

In Fig. 4 the stability areas for different parameters α are depicted in terms of k and s. The first diagram shows the case of unmodified shape function. The time step limit for rectangular mesh is equal to $2b/c$ and decreases for slope mesh. The maximum d/b ratio

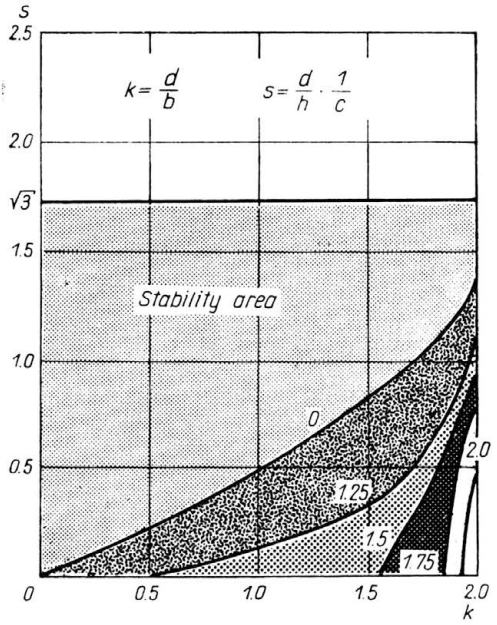

FIG. 4. Stability condition — quadrangular bar elements.

for the time step decreases to zero and $d_{\max} = 2/\sqrt{3}\,b$. When α is equal to 1.25, we have a stable scheme for any time step and the limit for d is equal to b and is independent of time. When the value of α increases, the maximum distance d is proportional to the time step.

Triangular elements

The properties of quadrangular element stability can be explained extensively after consideration of the system of triangular elements of a bar in axial vibration. Alternate space-time elements have oppositely-directed slope edges. The assumption of linear time and space distribution of displacements gives the values of coefficients:

$$\mathbf{A} = \frac{32EAhb}{4b^2-d^2} - \frac{4\varrho A(4b^2+d^2)}{h(2b+d)}, \quad \mathbf{D} = \mathbf{A}, \tag{4.9}$$

$$\mathbf{B} = \frac{2\varrho A(2b-d)}{h}, \quad \mathbf{C} = \mathbf{E} = \mathbf{F} = \mathbf{B}, \tag{4.10}$$

The eigenvalue problem of the condition (4.2) leads to the inequalities

$$(4.11) \qquad (1) \quad -2 \leqslant k \leqslant 0, \quad s > \sqrt{\frac{8}{2-k}\frac{k^2}{4+k^2}},$$

$$(4.12) \qquad (2) \quad 0 \leqslant k \leqslant 2, \quad s > \frac{k}{\sqrt{(2-k)}},$$

$$(4.13) \qquad (3) \quad -2 \leqslant k \leqslant 2, \quad s < \frac{2}{\sqrt{(2-k)}}.$$

The diagram of the relations (4.11)–(4.13) is shown in Fig. 5. It can be seen that for some values of the time step h the interval of the stability cannot be simply connected. The condition (3) of Eq. (4.13) describes the time step h for the stationary mesh (then $k = 0$):

$$(4.14) \qquad \left.\frac{ds}{dk}\right|_{k=0} = \frac{\sqrt{2}}{2}.$$

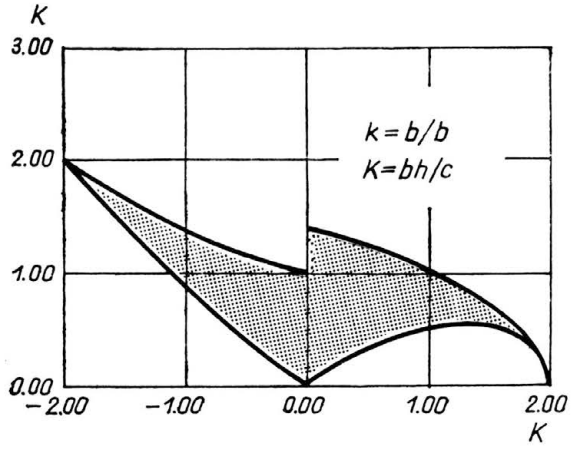

FIG. 5. Stability condition — triangular bar elements (first case).

Finally we have the critical value

$$(4.15) \qquad h_{cr} = \sqrt{2}b/c.$$

An identical condition is obtained for the central difference method.

When the space-time layers are reproducible (considering the sense of slope edges), the result of numerical searching of the stability area is depicted in Fig. 6. The stable region is bounded by the inequality

$$(4.16) \qquad \frac{\sqrt{2}}{2}k \leqslant s \leqslant \sqrt{2}, \quad 0 \leqslant k \leqslant 2.$$

However, the region of stability is not simply connected. Even small damping does not remove the instability inside the stable region. Moreover, the viscous damping does not change the critical time step although the upper limit of the parameter s slightly increases.

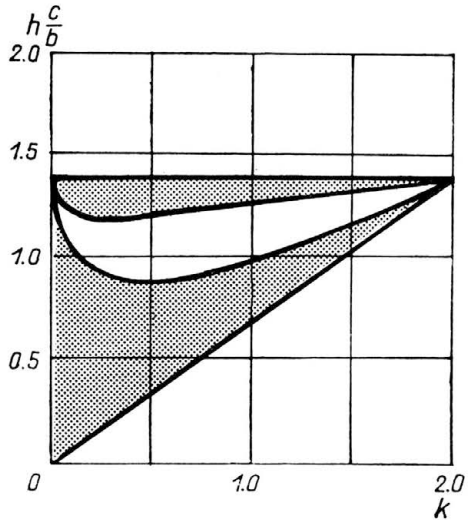

FIG. 6. Stability condition — triangular bar elements (second case).

Let us consider now modified shape functions for the virtual displacements

$$\tilde{\Phi}_i = L_i + \alpha(-2L_i^3 + 3L_i^2 - L_i + 2L_1L_2L_3), \tag{4.17}$$

$$\Phi_i = L_i^3 - \frac{3}{2}L_i^2 + \frac{3}{2}L_i - L_1L_2L_3. \tag{4.18}$$

The parameter α should be chosen to ensure the unconditional stability for the system built of such formulated elements. We have analyzed the sample mesh. The rectangle was divided into two triangular elements. The stepping scheme allows to determine the amplification matrix. The stability condition can be written then as

$$-1 \leqslant \frac{(K^2-1)\left(1-\frac{4\alpha}{45}\right)}{K^2\frac{\alpha}{90} - \frac{2}{45}\alpha + 1} \leqslant 1. \tag{4.19}$$

The parameter α can be easily determined:

$$\alpha \geqslant \begin{cases} 0, & \text{for} \quad 0 \leqslant K \leqslant \sqrt{2}, \\ \dfrac{30(K^2-2)}{3K^2-4}, & \text{for} \quad K \leqslant \sqrt{2}, \end{cases} \tag{4.20}$$

For comparison, the unconditionally stable case of the multiplex space-time element method was considered. We have the following recurrent formula:

$$\delta_{i+1} = \delta_{i-1} - \frac{2k^2(1-\alpha)-2}{k^2\alpha+1}\delta_i + \frac{2}{k^2\alpha+1}\frac{hF_i}{\varrho Ab}. \tag{4.21}$$

Equation (4.21) is unconditionally stable for $\alpha = 1.25$. The amplitude error obtained for α selected from the inequality (4.20) is significant in the case of greater time steps. The phase error, in contrary, is lower [31].

If we shift the argument in the inequality (4.20) by 2, we can eliminate the conditional inequality (4.20) receiving the value for α depending directly on k

$$\alpha = \frac{30k^2}{3k^2+2}. \tag{4.22}$$

A comparison of the phase error for selected time integration methods can also be found in [31].

5. Nostrationary partition — adaptive technique

Classical time integration methods cannot be successfully applied to some nonlinear problems. For example, standard time integration schemes applicable to viscoplasticity are unstable or inaccurate in the presence of cyclic loading and extremely fine meshes must be used in the finite element calculations in order to obtain reasonable representation of stress histories. The adaptation techniques based on the *a posteriori* error estimation have been intensively developed to increase the efficiency and accuracy of calculations [54–68]. There are two basic approaches of mesh refinement:

successive division of the element into smaller elements, increasing the number of joints (h-refinement),

moving the joints to regions of available rough partition (r-refinement).

The first way is inconvenient in time-dependent problems. Such are contact problems in dynamics. The initial phase is important and each approximation accumulates the error. The addition of new joints whose nodal parameters are interpolated does not increase accuracy remarkably while coarsening of the mesh always makes the solution worse. Stress waves in transient problems enforce frequent and total mesh modification, therefore such a procedure seems to be costly. The hierarchical procedure is based on the same principle.

The second way appears efficient. The refined zones are moved together with the stress field motion or other characteristic lines movement.

The full space-time approximation gives a natural way of mesh modification with a constant pattern of the mesh and unvaried number of nodal points and spatial elements. We apply this method in our work.

Error indicator

Many different error estimators have been suggested in the literature. However, we should select those satisfying the following requirements:

high speed of error estimation,

dimensionless form and normalized value, bounded $0 \leqslant e \leqslant 1$,

possibility of changing the feature that is to be tested; error estimation without necessity of stress calculation, based on the displacement may turn out to be efficient in motion investigation of the structure.

In our case we must optimize the distribution for a fixed number of elements. Let us denote $\bar{h}$ as a mesh size. The distribution of the error is given by the integral over the spatial domain (for example [61]).

$$\int_A \bar{h}(u_{xx}^2 + u_{yy}^2)dxdy = \text{constant}. \tag{5.1}$$

Modifying the relation (5.1) due to the interpolation formulas, we obtain the error measure for a joint i:

$$e_i = \left[\sum_k \left(\int_A \sum_m \sum_j N^j_{,k} N^j_{,k} u^j_k dA\right)^2\right]^{1/2}, \tag{5.2}$$

j denotes joint numbers in an element m to which the node i belongs. u^j_k is the displacement k of the joint j. Since the shape functions N are linear, the derivatives $N_{,i}$ are constant and the form (5.2) can be given explicitly what considerably increases the efficiency.

Algorithm of mesh modification

The following steps describe the mesh geometry modification: 1. Calculation of the nodal values of the error. 2. Normalization of nodal errors. 3. Calculation of movement components for a joint. New coordinates are computed as a position of the center of gravity of all joints being in direct connection with the considered joint. The distance of a joint translation in one step counted in Sect. 3 is always shorter than the average element spatial size h in surrounding elements. To avoid loss of stability, we must correlate the joint movement distance d with the time step Δt, wave speed c and element edge b (Fig. 6).

6. Nonlinear problems

We consider the continuous body that occupies the domain $\mathscr{B}_0$ in the initial configuration. $\overline{\mathscr{B}}_0$ ia a subdomain of E_3. By $\mathscr{B}_0$ we denote the interior of this domain and by $\partial\mathscr{B}_0$ its boundary which is the sum of $\partial\mathscr{B}_{0t}$ and $\partial\mathscr{B}_{0u}$ (Fig. 7). We use the *total Lagrangian* formulation X to define deformation and motion of the material in the theory of finite deformations. Dynamic variables applied in the formulation, i.e., the vector displacement field $\mathbf{u}$, body forces $\varrho_0\mathbf{f}_0$, symmetric Piola–Kirchhoff stress tensor field $\mathbf{T}$ and Green–

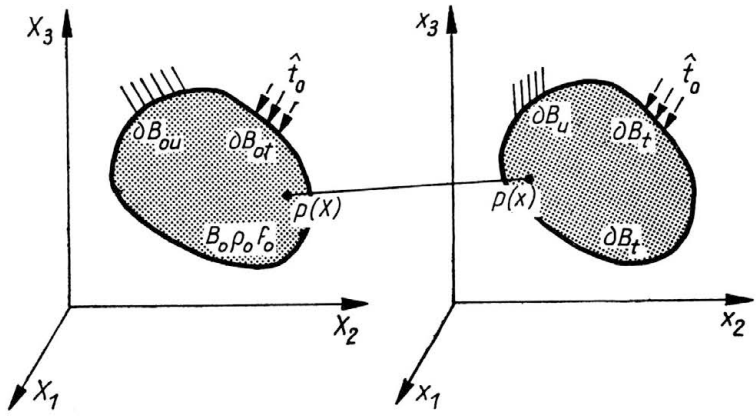

FIG. 7. Projection of the material point after deformation.

Lagrange strain tensor $\mathbf{E}$ are defined in the Cartesian product $\mathscr{B}_0 \times [0, T]$. The vector field of surface forces $\hat{t}_0$ are defined in $\partial\mathscr{B}_0 \times [0, T]$. The actual configuration is defined by the coordinate system $\mathbf{x}$, domains $\mathscr{B}$, $\partial\mathscr{B}_t$, $\partial\mathscr{B}_u$, body forces $\varrho\mathbf{f}$ and surface forces $\hat{\mathbf{t}}$. All the functions are sufficiently smooth. If we use the same Cartesian coordinates (straight-line and orthogonal) in the description of initial and actual configuration, then the strain is represented by the Green tensor in the form [53]

$$E_{ij}(\mathbf{X}, t) = \frac{1}{2}(u_{i,j}+u_{j,i}+u_{k,i}u_{k,j}), \tag{6.1}$$

$$u_i(\mathbf{X}, t) = x_i - X_i, \qquad \mathbf{X}, t \in \mathscr{B} \times [0, T].$$

Stresses in the actual configuration related to the initial one are defined by the II Piola–Kirchhoff tensor that is coupled with the Cauchy strain tensor σ:

$$\sigma_{ij}(\mathbf{X}, t) = \frac{\varrho}{\varrho_0}(\delta_{i\alpha}+u_{i,\alpha})(\delta_{j\beta}+u_{j,\beta})T_{\beta\alpha}, \tag{6.2}$$

$$\frac{\varrho}{\varrho_0} = \det|\delta_{ij}+u_{i,j}|.$$

The relation between the symmetric strain and stress tensor can be written as

$$T_{ij}(\mathbf{X}, t) = D_{ijkl}(\mathbf{X}, t, \mathbf{E}, \dot{\mathbf{T}}, \dot{\mathbf{E}}, \ldots)E_{kl}, \qquad X, t \in \mathscr{B}_0 \times [0, T], \tag{6.3}$$

where $\mathbf{D}$ describes the material properties. Constitutive equations are described in numerous references (for example [51, 53]). The coefficients are given explicitly in [48]. The equilibrium equation in the Lagrange coordinates based on the second Piola–Kirchhoff tensor is written in a known form:

$$[T_{jk}(\delta_{ik}+u_{i,k})]_{,j}+\varrho_0(f_{0i}-\ddot{u}_i) = 0, \qquad \mathbf{X}, t \in \mathscr{B}_0 \times [0, T]. \tag{6.4}$$

The unique solution requires the boundary conditions:

static conditions

$$\hat{t}_{0i} = T_{jk}(\delta_{ik}+u_{i,k})\nu_{0j}, \qquad \mathbf{X}, t \in \partial\mathscr{B}_{0t} \times [0, T], \tag{6.5}$$

displacement condition

$$u_i = \hat{u}_i, \qquad \mathbf{X}, t \in \partial\mathscr{B}_0 \times [0, T], \tag{6.6}$$

the initial conditions

$$u_i = u_i^0, \qquad \dot{u}_i = v_i^0, \qquad \mathbf{X}, t \in \bar{\mathscr{B}}_0 \times \{0\} \tag{6.7}$$

(ν_0 is the outward normal to the element surface $\partial\mathscr{B}_{0t}$).

We can pass to the global formulation. Let us multiply Eq. (6.4) by the virtual variation of the displacement function

$$\delta\mathbf{u}(\mathbf{X}, t) = \begin{cases} \text{any}, & \mathbf{X}, t \in \partial\mathscr{B}_{0u} \times [0, T], \\ \mathbf{0}, & \mathbf{X}, t \in (\bar{\mathscr{B}}_0 - \partial\mathscr{B}_{0u}) \times [0, T] \end{cases} \tag{6.8}$$

and integrate over the space-time domain. Then we have

$$\int_0^{t_1}\int_{\mathscr{B}_0} \varrho_0(f_{0i}\delta u_i+\dot{u}_i\delta\dot{u})\,d\mathscr{B}_0\,dt+\int_0^{t_1}\int_{\partial\mathscr{B}_0} \hat{t}_{0i}\delta u_i\,d(\partial\mathscr{B}_0)dt \tag{6.9}$$

$$+\int_{\mathscr{B}_0} \varrho\dot{u}\delta u_i\,d\mathscr{B}\Big|_0^{t_1} = \int_0^{t_1}\int_{\mathscr{B}_0} T_{ij}\delta E_{ij}\,d\mathscr{B}_0\,dt, \qquad t_1 \in [0, T].$$

After discretization of the space-time domain the static and geometrical quantities are described according to the nodal parameters of the space-time element:

$$
\begin{aligned}
u_i(\mathbf{X}, t) &= \Phi_{i\alpha}(\mathbf{X}, t) r_\alpha, \qquad \delta u_i(\mathbf{X}, t) = \Phi_{i\alpha}(\mathbf{X}, t)\delta r_\alpha, \\
\dot{u}_i(\mathbf{X}, t) &= \dot{\Phi}_{i\alpha}(\mathbf{X}, t) r_\alpha, \qquad \delta \dot{u}_i(\mathbf{X}, t) = \dot{\Phi}_{i\alpha}(\mathbf{X}, t)\delta r_\alpha, \\
E_{ij}(\mathbf{X}, t) &= [{}'B_{ij\alpha} + {}''B_{ij\alpha}(r_\beta)] r_\alpha, \\
\delta E_{ij}(\mathbf{X}, t) &= [{}'B_{ij\alpha} + 2\,{}''B_{ij\alpha}(r_\beta)]\delta r_\alpha, \\
T_{ij}(\mathbf{X}, t) &= D_{ijkl}[{}'B_{kl\alpha} + {}''B_{kl\alpha}(r_\beta)] r_\alpha, \qquad i, j, k, l = 1, 2, 3, \qquad \alpha = 1, 2, \ldots, N,
\end{aligned} \tag{6.10}
$$

where

$$
\begin{aligned}
{}'B_{ij\alpha} &= \frac{1}{2}(\Phi_{i\alpha,j} + \Phi_{j\alpha,i}), \\
{}''B_{ij\alpha} &= \frac{1}{2}\Phi_{k\alpha,i}\Phi_{k\beta,j} r_\beta.
\end{aligned} \tag{6.11}
$$

Applying the approximation formulas (6.10) to Eq. (6.9) we have

$$
\sum_{e=1}^{E} \{[{}^{(\mathrm{con})}K^e_{\alpha\beta} + {}^{(u)}K^e_{\alpha b} + {}^{(\sigma)}K^e_{\alpha\beta} - M^e_{\alpha\beta}] r_\beta - R^e_\alpha\} = 0, \tag{6.12}
$$

where

$$
\begin{aligned}
{}^{(\mathrm{con})}K^e_{\alpha\beta} &= \int\!\!\int_{\Omega_e} D^e_{ijkl}, B^e_{ij\alpha}, B^e_{kl\beta}\, d\Omega, \\
{}^{(u)}K^e_{\alpha\beta} &= \int\!\!\int_{\Omega_e} D^e_{ijkl}\, {}''B^e_{ij\alpha}\, {}''B^e_{kl\beta}\, d\Omega, \\
{}^{(\sigma)}K^e_{\alpha\beta} &= 2\int\!\!\int_{\Omega_e} D^e_{ijkl}({}'B^e_{kl\alpha} + {}''B^e_{kl\alpha})\, {}''B^e_{ij\beta}\, d\Omega = \int\!\!\int_{\Omega_e} T^e_{kl}\Phi^e_{i\alpha,k}\Phi^e_{i\beta,l}\, d\Omega, \\
M^e_{\alpha\beta} &= \int\!\!\int_{\Omega} \varrho^e_0 \dot{\Phi}^e_{i\alpha}\dot{\Phi}^e_{i\beta}\, d\Omega, \\
R^e_\alpha &= \int\!\!\int_{\Omega_e} \varrho^e_0 f^e_{0i}\Phi^e_{i\alpha}\, d\Omega + \int\!\!\int_{\partial\Omega_{te}} t^e_{0i}\Phi^e_{i\alpha}\, d(\partial\Omega) + \int_{\mathscr{B}_{0e}} \varrho^e_0 \dot{u}^e_i \Phi^e_{i\alpha}\, d\mathscr{B}_0 \Big|_{t^e_{\mathrm{init}}}^{t^e_{\mathrm{end}}}.
\end{aligned} \tag{6.13}
$$

In analogy to the terminology used in the classical finite element method [51], the matrices ${}^{(\mathrm{con})}K^e_{\alpha\beta}$, ${}^{(u)}K^e_{\alpha\beta}$, ${}^{(\sigma)}K^e_{\alpha\beta}$ and $M^e_{\alpha\beta}$ are called the constitutive stiffness matrix, displacement stiffness matrix, stress stiffness (geometrical) matrix and mass matrix, respectively. The expression

$$
K^e_{\alpha\beta} = {}^{(\mathrm{con})}K^e_{\alpha\beta} + {}^{(u)}K^e_{\alpha\beta} + {}^{(\sigma)}K^e_{\alpha\beta} - M^e_{\alpha\beta} \tag{6.14}
$$

is the space-time element stiffness matrix.

6.1. Incremental procedure

Let us consider a space-time layer $t_n \leqslant t \leqslant t_n + \Delta t$. We can write the work equilibrium equation at time t:

$$
\int_{{}^t\mathscr{B}} ({}^t_{t_n}\mathbf{T}_{ij}\,\delta\, {}^t_{t_n}\mathbf{E}_{ij} + {}^t\varrho\, {}^t_{t_n}\ddot{\mathbf{u}}_i\,\delta\, {}^t_{t_n}\mathbf{u}_i)\, {}^t d\mathscr{B} = {}^t\mathscr{R}, \tag{6.15}
$$

where

${}^t_{t_n}\mathbf{T}_{ij}$ — II Piola–Kirchhoff stress tensor in time t related to the configuration in t_n,

${}^t_{t_n}\mathbf{E}_{ij}$ — Green–Lagrange strain tensor,

${}^t\varrho$ — mass density,

${}^t\mathscr{R}$ — virtual work of external loads

$$ {}^t\mathscr{R} = \int_{{}^t\mathscr{B}} {}^t\mathbf{f}_i \delta\mathbf{u}_i \, {}^t d\mathscr{B} + \int_{{}^t\partial\mathscr{B}_\sigma} {}^t\hat{\mathbf{t}}_i \delta\mathbf{u}_i \, {}^t d(\partial\mathscr{B}), \tag{6.16} $$

${}^t\mathbf{f}_i$, ${}^t\hat{\mathbf{t}}_i$ — body and surface force coefficients at time t.

Further we apply the incremental decomposition

$$ {}^t_{t_n}\mathbf{T}_{ij} = {}^{t_n}_{t_n}\mathbf{T}_{ij} + \Delta\mathbf{T}_{ij} = {}^{t_n}\mathbf{T}_{ij} + \Delta\mathbf{T}_{ij}, \tag{6.17} $$

$$ {}^t_{t_n}\mathbf{E}_{ij} = \Delta\mathbf{E}_{ij}, \tag{6.18} $$

$$ {}^t_{t_n}\mathbf{u}_i = {}^{t_n}_{t_n}\mathbf{u}_i + \Delta\mathbf{u}_i \tag{6.19} $$

and the constitutive relation

$$ \Delta\mathbf{T}_{ij} = {}_{t_n}\mathbf{C}_{ijkl}\Delta\mathbf{E}_{kl}. \tag{6.20} $$

Now we can integrate Eq. (6.15) over the time interval $[t_n, t_{n+1}]$. Further we use the matrix notation since it is applicable in computational procedures. As a result we have

$$ \left[\int_{\Omega_i}\int (\mathbf{D}\Phi)^T C \mathbf{D}\Phi \, d\Omega_i + \int_{\Omega_i}\int (\mathbf{D}_N\Phi)^T \tau \mathbf{D}_N\Phi \, d\Omega_i - \int_{\Omega_i}\int \left[\frac{\partial\Phi}{\partial t}\right]^T \varrho \frac{\partial\Phi}{\partial t} \, d\Omega_i\right] \Delta q $$
$$ = F - \int_{\Omega_i}\int (\mathbf{D}\Phi)^T \hat{\tau} \, d\Omega_i + \left[\int_{\Omega}\int \left[\frac{\partial\Phi}{\partial t}\right]^T \varrho \frac{\partial\Phi}{\partial t} \, d\Omega_i\right] q, \tag{6.21} $$

where $\mathbf{D}$ and $\mathbf{D}_N$ are the differential operators for the linear and nonlinear part of considerations, respectively, τ is the stress matrix and $\hat{\tau}$ is the stress vector or, in the short form,

$$ (\mathbf{K}^i_L + \mathbf{K}^i_{NL} + \mathbf{M}^i)\Delta\mathbf{q} = \Delta\mathbf{F}^i - (\mathbf{F}^i_N + \mathbf{M}^i q^i - \mathbf{F}^i). \tag{6.22} $$

7. Examples of applications

Numerical examples prove the efficiency of the STEM. Problems are modelled by simple space-time elements. Linear shape functions, however, allow to obtain an accuracy comparative with FEM solutions. Adaptive techniques applied to simple test problems enhance the accuracy, especially increasing the higher mode vibrations. In further examples nonlinear material properties are included.

Cantilever plate

We solved the plate of dimensions $L \times L/2$, firmly supported at one end, subjected to a Heaviside point force placed in the middle of the free end. A successively condensed triangular mesh, starting from 2×1 squares subdivided into triangles, enables to obtain higher accuracy. The results are compared with the FEM solutions and modal analysis (Table 1). It should be emphasized that tetrahedral space-time elements of constant strain were used.

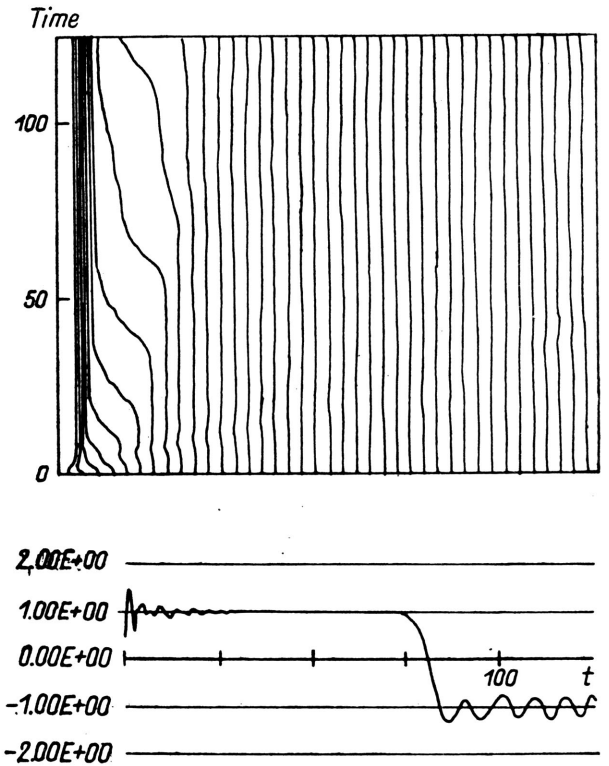

FIG. 8. Mesh adaptation — impulse load.

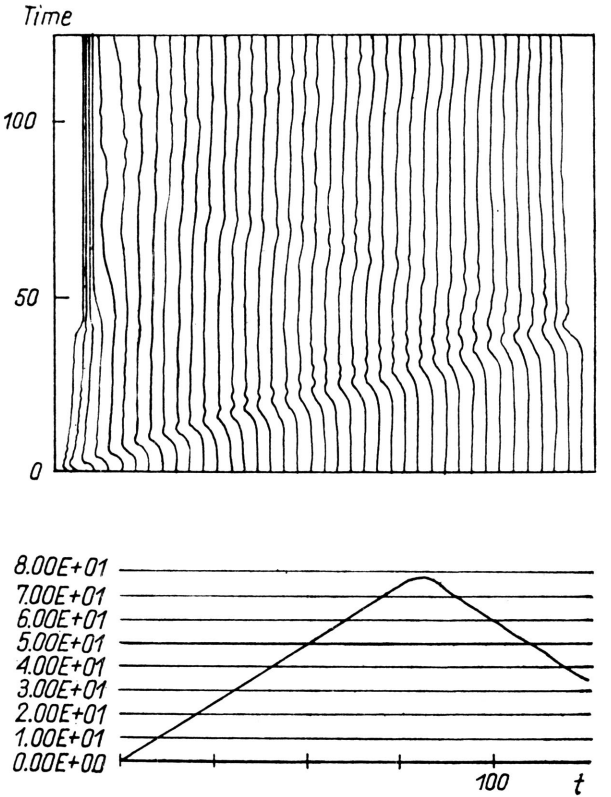

FIG. 9. Mesh adaptation — Heaviside load.

Table 1.

Partition	No. of joints	$\frac{wD}{QL^2}$	$\frac{\omega}{\sqrt{D/\varrho t L^4}}$
2×1	6	0.564	4.84
4×2	15	0.953	3.97
8×4	45	1.277	3.36
experiment			3.42*
Ritz method			3.47*
2×1 (4 triangles) — modal FEM analysis			3.39*
4×2 (16 triangles) — modal FEM analysis			3.44*
double static deflection		1.472	

* [8] second edition

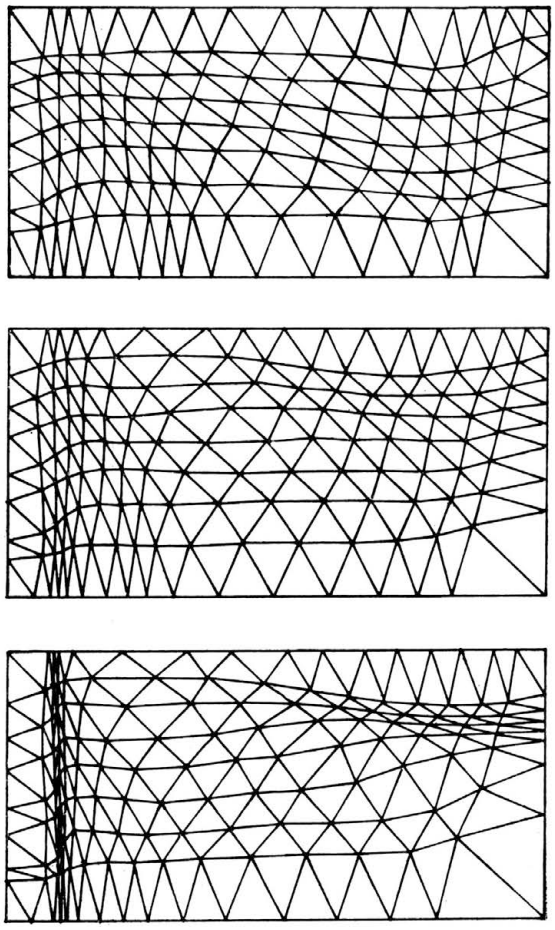

FIG. 10. Mesh adaptation under moving load — three stages after 1 cm, 2 cm and 3 cm path of total dimension = 32 cm.

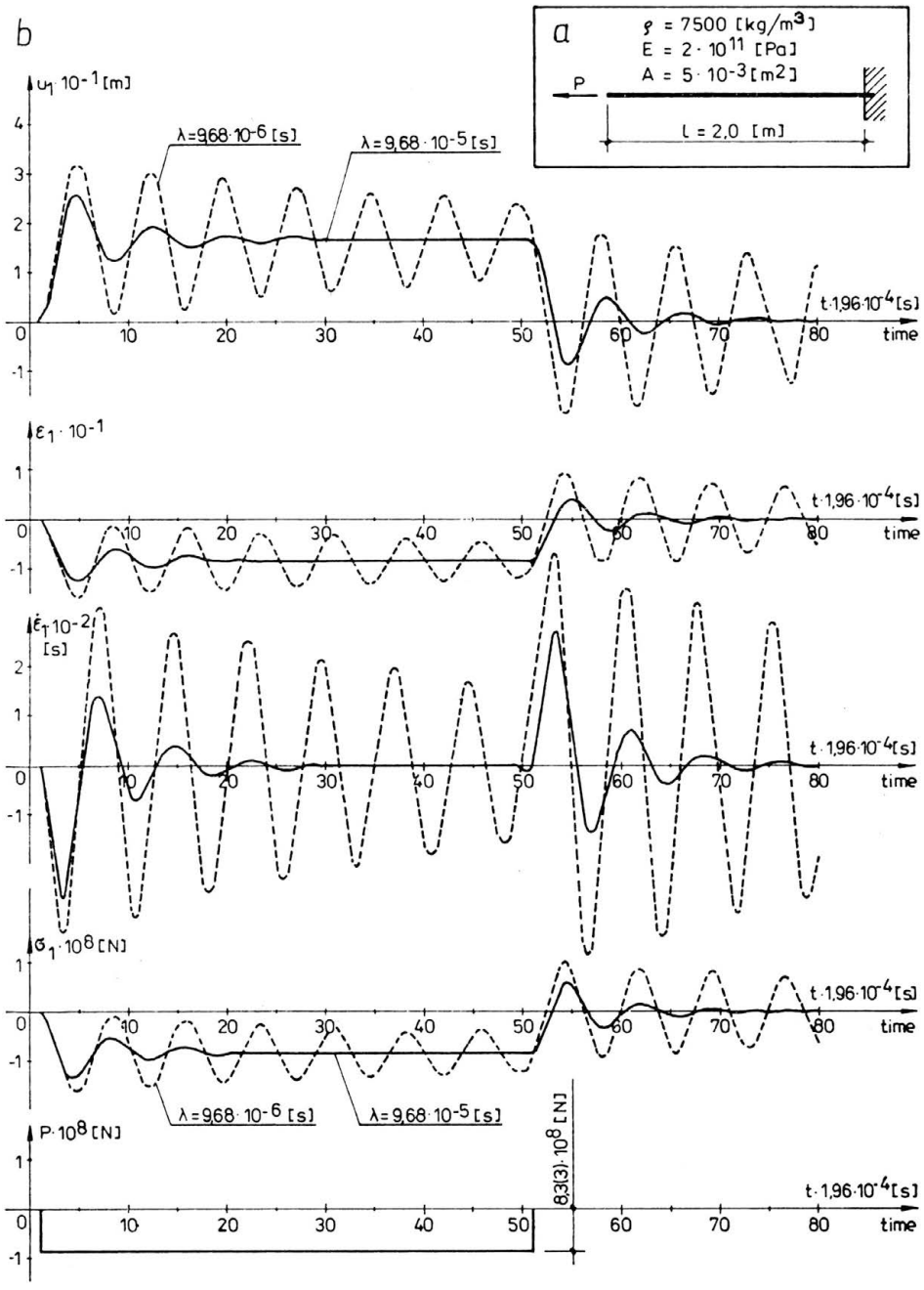

FIG. 11. Nonlinear vibrations of a bar.

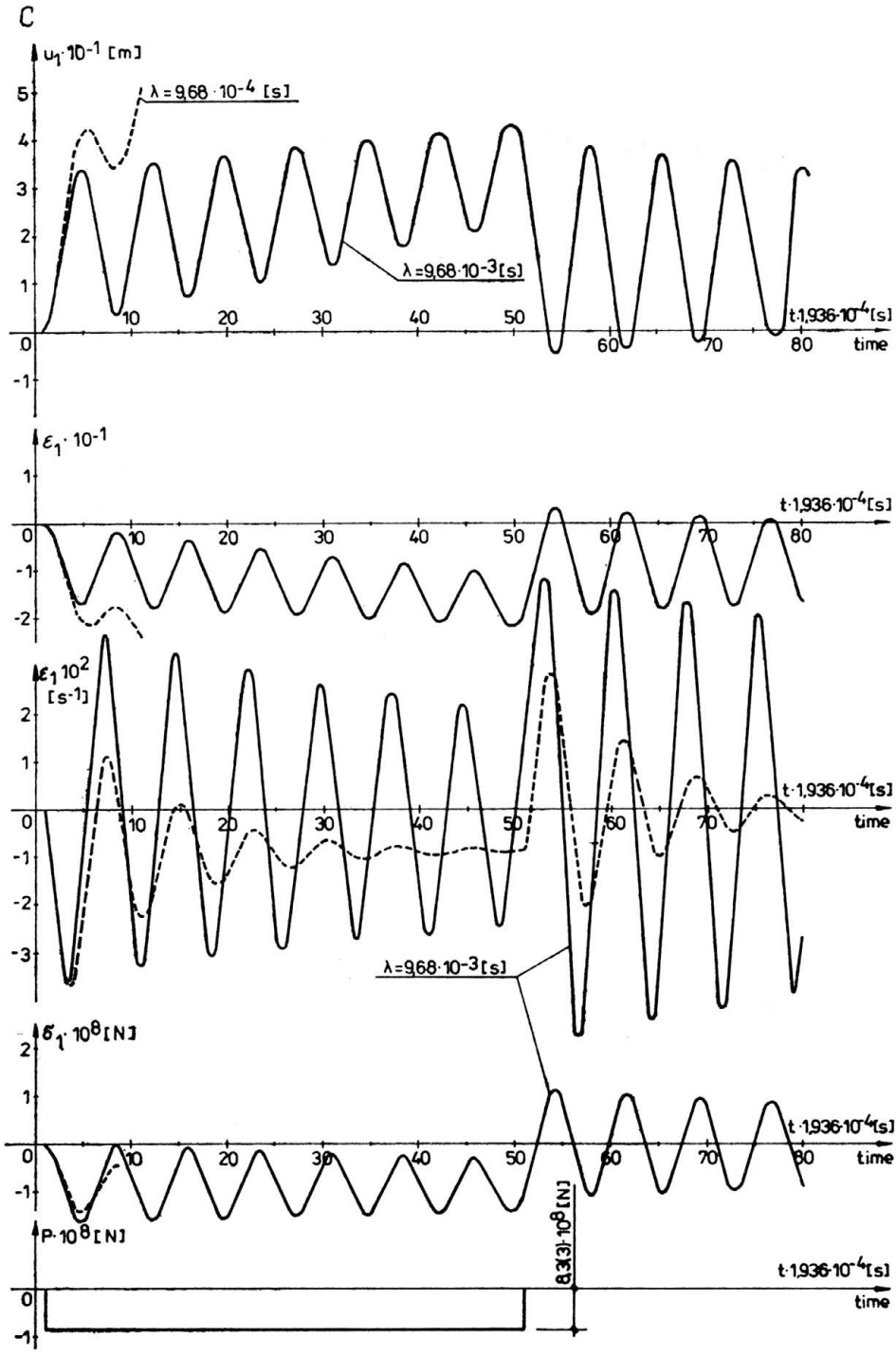

[Fig. 11c]

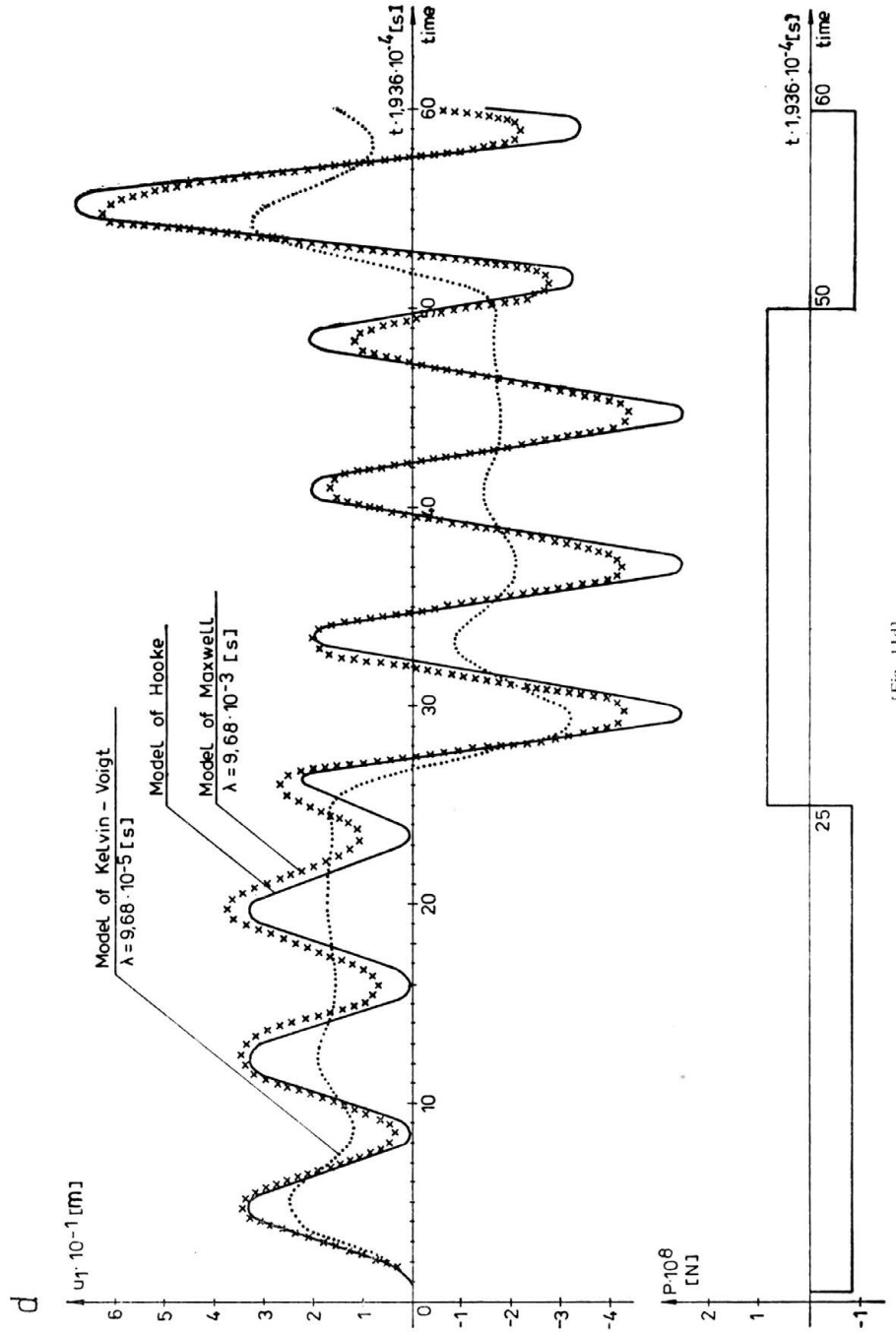

[Fig. 11d]

Vibrating bar self-adaptive mesh

The bar divided into 40 spatial elements is supported at the end. The impulse force is placed to the free end. The partition in space is adapted due to the assumed error criterion. The spatial partition as a function of time is depicted in Fig. 8. We can notice the joint movement at the moment of a passing wave. Below we have the diagram of displacements in time of the subjected joint. In Fig. 9 the identical task is depicted with the only difference that the Heaviside force is applied to the end joint.

Plane starin structure — adaptive mesh

We treated the plane strain rectangular domain subjected to a travelling point force. Joints go to the vertical band of much higher stress gradients. An initially regular mesh of 8×16 squares is deformed and three stages are presented in Fig. 10.

Visco-elastic bar

Longitudinal vibrations of a bar were investigated but the material was a viscoelastic one. In Fig. 11 (a) the sample bar is depicted together with all the necessary material data. Figure 11 (b) presents displacements in time in the case of the Kelvin–Voigt material and Fig. 11 (c) deals with the Maxwell material. Displacement u_1, strain ε_1, speed of strain $\dot{\varepsilon}_1$, stress σ_1 and the subjecting force P for different material models are presented in Fig. 11 (d).

8. Future directions

In the present work we did not broadly discuss the paper by HUGHES and HULBERT [2]. The discontinuous in time method of approximation allows to obtain unconditionally stable schemes resulting from the least squares analysis. The portion of accumulated energy is distributed on joints in each time layer. However, the accuracy has not been proved in the paper. In the case of large time steps we can expect divergency. In any case the proposed method should be verified with the use of simplex-shaped elements. Then the best features of both approaches would be joined.

The unconditional stability is still the main disadvantage of the method. Each improvement to overcome this inconvenience would be precious.

The deficiency of the commercial computer codes makes widespread use by engineers impossible. For the same reason the experiments and practical results are still poor.

References

1. J. H. CUSHMAN, *Difference schemes or element schemes*?, Int. J. Num. Meth. Engng., **14**, 1643–1651, 1979.
2. T. J. R. HUGHES, G. M. HULBERT, *Space-time element methods for elastodynamics: formulations and error estimates*, Comp. Meth. Appl. Mech. Engng., **66**, 339–363, 1988.

3. I. FRIED, *Finite element analysis of time dependent phenomena*, AIAA J., **7**, 1170–1172, 1969.
4. J. T. ODEN, *A generalized theory of finite elements, II. Applications*, Int. J. Num. Meth. Engng., **1**, 247–259. 1969.
5. J. H. ARGYRIS, D. W. SCHARPF, *Finite element in space and time*, Nucl. Engng. Design, **10**, 456–469, 1969.
6. J. H. ARGYRIS, D. W. SCHARPF, *Finite element in time and space*, Aero. J. RAS, **73**, 1041–1044, 1969.
7. J. H. ARGYRIS, A. S. L. CHAN, *Application of finite elements in space and time*, Ing. Arch., **41**, 235–257, 1972.
8. O. C. ZIENKIEWICZ, *The finite element method*, McGraw-Hill, London 1977.
9. O. C. ZIENKIEWICZ, *Finite elements in the time domain*, in: State-of-the-Art Surveys on Finite Element Technology, ed. A. K. NOOR, W. D. PILKEY, ASME, 1983.
10. Z. KĄCZKOWSKI, *The method of finite space-time finite elements in dynamics of structures*, J. Techn. Phys., **16**, 69–84, 1975.
11. Z. KĄCZKOWSKI, *The method of time dependent finite elements*, Arch. Inżyn. Lądowej, **22**, 3, 365–378, 1976 [in Polish].
12. Z. KĄCZKOWSKI, *General formulation of stiffness matrix for space-time finite elements*, Arch. Inżyn. Lądowej, **25**, 351–357, 1979.
13. Z. KĄCZKOWSKI, M. WITKOWSKI, *Accounting for external damping in the method of finite space-time elements*, Arch. Inżyn. Lądowej, **23**, 3, 243–254, 1977 [in Polish].
14. Z. KĄCZKOWSKI, Z. WITKOWSKIA, *Transfer matrix in the method of time-space finite elements*, Arch. Inżyn. Lądowej, **24**, 1, 59–66, 1978 [in Polish].
15. Z. KĄCZKOWSKI, M. ŻYSZKO, *Flexural vibrations of bars by the method of time-space finite elements*, Arch. Inżyn. Lądowej, **24**, 1, 67–78, 1978 [in Polish].
16. J. BRZEZIŃSKI, M. PIETRZAKOWSKI, *The testing of non-stationary vibrations of simple hybrid system by the space-time finite elements*, Arch. Bud. Maszyn. **26**, 4, 511–526, 1979 [in Polish].
17. M. WITKOWSKI, *Space-time element method as a series of statical problems*, Arch. Inżyn. Lądowej, **27**, 3, 727–734, 1980 [in Polish].
18. Z. KACPRZYK, *Vibration analysis of a chimney swallow with a seismic load*, Arch. Inżyn. Lądowej, **27**, 3, 501–516, 1981 [in Polish].
19. H. MALSCH, *Zur Berechnung von Durchsenkungen eines Balkens unter Folgen von wandernden Lasten mit finiten Raum-Zeit-Elementen*, Ingeneur-Archiv, **47**, 105–115, 1978.
20. H. MALSCH, *Die Berechnung nichtlinear Schwingungen mit finiten Raum-Zeit-Elementen*, Ingenieur-Archiv, **47**, 349–361, 1978.
21. Z. KACPRZYK, *Space-time superelement*, Arch. Inżyn. Lądowej, **28**, 1–2, pp. 47–55, 1982 [in Polish].
22. Z. KĄCZKOWSKI, J. LANGER, *Synthesis of the space-time finite element method*, Arch. Inżyn. Lądowej, **26**, 11–17, 1980.
23. J. LANGER, *Spurious damping in computer-aided solutions of the equations of motion*, Arch. Inżyn. Lądowej, Lądowej, **25**, 3, 359–369, 1979 [in Polish].
24. W. CYGANECKI, *Criteria to select dimensions of a space-time element*, Arch. Inżyn. Lądowej, **25**, 3, 389–397, 1979 [in Polish].
25. W. CYGANECKI, *On the dimensions of the space-time elements*, Arch. Inżyn. Lądowej, **26**, 4, 717–726, 1980 [in Polish].
26. Cz. BAJER, *Modelling of dynamic systems by the use of non-rectangular space-time elements*, Prace Nauk. Polit. Świętokrzyskiej, Budown., 18, 5–10, 1984 [in Polish].
27. Z. KACPRZYK, *On the application of weighting functions in the space-time finite element method*, Prace Nauk. Polit. Warszawskiej, Budown., 85, 83–95, 1984 [in Polish].
28. Z. KACPRZYK, T. LEWIŃSKI, *Comparison of some numerical integration methods for the equations of motion of the systems with a finite number of degrees of freedom*, Engng. Trans., **31**, 213–240, 1983.
29. J. PELC, *Nonlinear shape functions in the space-time element method*, Arch. Inżyn. Lądowej, **30**, 1, 53–63, 1984 [in Polish].
30. C. I. BAJER, *Notes on the stability of non-rectangular space-time finite elements*, Int. J. Num. Meth. Engng., **24**, 1721–1739, 1987.

31. Cz. Bajer, *Unconditionally stable variant of the space-time element method*, Arch. Inżyn. Lądowej, **33**, 3, 287–295, 1987 [in Polish].
32. A. Podhorecki, *Stability of solutions in the space-time element method*, Engng. Trans., 1988 (in print) [in Polish].
33. Z. Kączkowski, *On using of non-rectangular space-time elements*, Mech. Teret. Stos., **21**, 4, 531–554, 1983 [in Polish].
34. M. Witkowski, *On the space-time in structural dynamics*, Prace Nauk. Polit. Warszawskiej, Budown., 80, 1983 [in Polish].
35. Z. Kączkowski, A. Borkowski, *Zur numerischen Stabilität der Verfahrens der Raum-Zeit-Elemente mit schrägen Rändern*, ZAMM, **68**, 387–388, 1985.
36. Z. Kączkowski, *On the solution of a complete dynamic contact problem by the space-time element method*, Zesz. Nauk. Polit. Poznańskiej, Budown. Lądowe, **31**, 63–72 [in Polish].
37. M. Witkowski, *Triangular time-space elements in analysis of wave problem*. Engng. Trans., **33**, 4, 549–564, 1985 [in Polish].
38. Cz. Bajer, *Triangular and tetrahedral space-time finite elements in vibration analysis*, Int J. Num. Meth. Engng., **23**, 2031–2048, 1986.
39. A. Cella, M. Lucchiesi, G. Pasquinelli, *Space-time elements for the shock wave propagation problem*, Int. J. Num. Meth. Engng., **15**, 1457–1488, 1980.
40. A. Podhorecka, *The space-time finite element method in the geometrically nonlinear problems*, Mech. Teoret. Stos., 1988 (in print) [in Polish].
41. A. Podhorecki, *The space-time finite element method in nonlinear continuum mechanics*, Prace Nauk. Akademii Techn.-Roln. w Bydgoszczy, Budown., **24**, 21–29, 1987 [in Polish].
42. Z. Kączkowski, *On the application of the space-time element method to the heat conduction problem*, Arch. Inżyn. Lądowej, **31**, 3, 361–373, 1985 [in Polish].
43. J. R. Yu, T. R. Hsu, *The solution of diffusion-convection equation by the space-time finite element method*, Int. J. Num. Meth. Engng., **23**, 737–750, 1986.
44. J. R. Yu, T. R. Hsu, *Ananysis of heat conduction in solids by space-time finite element method*, Int. J. Num. Meth. Engng., **21**, 1985.
45. H. Nguyen, J. Reynen, *A space-time least square finite element scheme for advection-diffusion equations*, Comp. Meth. Appl. Mech. Engng., **42**, 331–342, 1984.
46. W. Köhler, J. Pittr, *Calculation of transient temperature fields with finite elements in space and time dimensions*, Int. J. Num. Meth. Engng., **8**, 625–631, 1974.
47. Z. Kączkowski, *On variational principles in thermoelasticity*, Bull. Acad. Polon. Sci., Ser. Sci. Tech., 5–6, pp. 81–86, 1982.
48. A. Podhorecki, *Space-time element method in certain viscoelastic problems*, Prace Nauk. Akademii Techn.-Roln. w Bydgoszczy (in print) [in Polish].
49. A. Podhorecki, A. Podhorecka, *Viscoelastic time-space element*, Engng. Trans., **33**, 1–2, pp. 3–22, 1985 [in Polish].
50. A. Podhorecki, *The viscoelastic space-time element*, Comp. and Struct., **23**, 535–544, 1986.
51. M. Kleiber, *Finite element method in nonlinear continuum mechanics*, PWN, Warszawa-Poznań 1985 [in Polish].
52. W. Nowacki, *Dynamics of structures*, Arkady, Warszawa 1972 [in Polish].
53. Y. C. Fung, *Foundations of solid mechanics*, Prentice-Hall, Eng. Cliffs, New Jersey 1965.
54. D. W. Kelly, R. J. Milles, J. A. Reises, *A posteriori error estimates in finite difference techniques*, J. Comp. Phys., **74**, 214–232, 1988.
55. O. C. Zienkiewicz, D. W. Kelly, J. Gago, I. Babuska, *Hierarchical finite element approaches, error estimates and adaptive refinement*, MAFELAP, conf., Brunel University, 313–346.
56. K. Miller, R. N. Miller, *Moving finite elements. I*, SIAM J. Num. Anal., **18**, 1091–1032, 1981.
57. K. Miller, *Moving finite elements. II*, SIAM J. Num. Anal., **18**, 1033–1057, 1981.
58. Z-B. Kuang, S. N. Alturi, *Temperature field due to a moving heat source: a moving mesh finite element analysis*, J. Appl. Mech., **52**, 274–280, 1985.
59. R. J. Gu, *Moving finite element analysis for the elastic beams in contact problems*, Comp. and Struct., **24**, 571–579, 1986.

60. R. SANDERS, *Moving grid method for nonlinear hyperbolic conservation laws*, SIAM J. Num. Anal., **22**, 713–728, 1985.
61. R. LÖHNER, *An adaptive finite element scheme for transient problems in CFD*, Comp. Meth. Appl. Mech. Engng., **61**, 323–338, 1987.
62. P. DEVLOO, J. T. ODEN, T. STROUBOULIS, *Implementation of an adaptive refinement technique for the SUPG algorithm*, Comp. Meth. Appl. Mech. Engng., **61**, 339–358, 1987.
63. L. DEMKOWICZ, J. T. ODEN, *Mesh optimization method based on a minimization of interpolation error*, Int. J. Engng. Sci., **24**, 55–68, 1986.
64. L. DEMKOWICZ, *Adaptive finite element methods*, Prace Nauk. Polit. Krakowskiej, 1986 [in Polish].
65. J. M. BASS, J. T. ODEN, *Adaptive finite element method for a class of problems in viscoplasticity*, Int. J. Eng. Sci., **25**, 623–653, 1987.
66. A. ADJERID, J. E. FLAHERTY, *A moving finite element method with error estimation and refinement for one-dimensional time-dependent partial differential equations*. SIAM J. Num. Anal., **23**, 778–796, 1986.
67. H. E. FEBRES-CEDILLO, M. A. BHATTI, *A simple strain energy based finite element mesh refinement scheme*, Comp. and Struct., **28**, 523–533, 1988.
68. C. I. BAJER, *Adaptive mesh in dynamic problems by the space-time approach*, Comp. Struct., **33**, 319–325, 1989.

POLISH ACADEMY OF SCIENCES
INSTITUTE OF FUNDAMENTAL TECHNOLOGICAL RESEARCH
and
DEPARTMENT OF CIVIL ENGINEERING
ACADEMY OF TECHNOLOGY AND AGRICULTURE, BYDGOSZCZ

Received November 8, 1988.